

This is a repository copy of *3D Modeling of craniofacial ontogeny and sexual dimorphism in children*.

White Rose Research Online URL for this paper:
<https://eprints.whiterose.ac.uk/170997/>

Version: Accepted Version

Article:

Smith, Olivia A.M., Nashed, Youssef S.G., Duncan, Christian et al. (3 more authors) (2020) 3D Modeling of craniofacial ontogeny and sexual dimorphism in children. *Anatomical Record*. ISSN 1932-8494

<https://doi.org/10.1002/ar.24582>

Reuse

Items deposited in White Rose Research Online are protected by copyright, with all rights reserved unless indicated otherwise. They may be downloaded and/or printed for private study, or other acts as permitted by national copyright laws. The publisher or other rights holders may allow further reproduction and re-use of the full text version. This is indicated by the licence information on the White Rose Research Online record for the item.

Takedown

If you consider content in White Rose Research Online to be in breach of UK law, please notify us by emailing eprints@whiterose.ac.uk including the URL of the record and the reason for the withdrawal request.

1 **3D Modelling of Craniofacial Ontogeny and Sexual Dimorphism in Children**

2 Olivia A. M. **Smith**¹, Youssef S.G. **Nashed**⁴, Christian **Duncan**², Nick **Pears**³, Antonio
3 **Profico**⁵, Paul **O'Higgins**^{1, 5}

4 1. Hull York Medical School, University of York, York, UK, YO10 5DD

5 2. Dept. of Plastic Surgery, Alder-Hey Hospital, Liverpool, UK, L12 2AP

6 3. Department of Computer Science, University of York, York, UK YO10 5GH

7 4. Stats Perform, Chicago, IL, USA, 60601;

8 5. PalaeoHub, Dept. of Archaeology, University of York, York, UK YO10 5DD

9

10 **Corresponding author:**

11 Paul O'Higgins, BSc, MBBS, PhD, DSc
12 PalaeoHub,
13 Dept. of Archaeology and Hull York Medical School,
14 University of York,
15 York,
16 UK
17 YO10 5DD
18 paul.ohiggins@hyms.ac.uk
19 tel:+44 1904 328872

20

21 Financial Disclosure Statement: The authors have no interests to disclose

22 Short Running Head:

23 Craniofacial ontogeny and sexual dimorphism

24

25 Grant sponsor(s): __0____; Grant number(s): __0____.

26

27 **Abstract:**

28 **Background**

29 The range of normal variation of growth and development of the craniofacial region is
30 of direct clinical interest but incompletely understood. Here we develop a statistical
31 model of craniofacial growth and development to compare craniofacial ontogeny
32 between age groups and sexes and pilot an approach to modelling that is relatively
33 straightforward to apply in the context of clinical research and assessment.

34 **Methods**

35 The sample comprises head surface meshes captured using a 3dMD five-camera
36 system from 65 males and 47 females (range 3-20 years) from the *Headspace* project,
37 Liverpool, UK. The surface meshes were parameterised using 16 anatomical
38 landmarks and 59 semilandmarks on curves and surfaces. Modes and degrees of
39 growth and development were assessed and compared among ages and sexes using
40 Procrustes based geometric morphometric methods.

41 **Results**

42 Regression analyses indicate that 3-10 year olds undergo greater changes than 11-
43 20 year olds and that craniofacial growth and development differs between these age
44 groups. The analyses indicate that males extend growth allometrically into larger size
45 ranges, contributing substantially to adult dimorphism. Comparisons of ontogenetic
46 trajectories between sexes find no significant differences, yet when hypermorphosis is
47 accounted for in the older age group there is a significant residual sexual dimorphism.

48 **Conclusions.**

49 The study adds to knowledge of how adult craniofacial form and sexual dimorphism
50 develop. It was carried out using readily available software which facilitates replication
51 of this work in diverse populations to underpin clinical assessment of deformity and
52 the outcomes of corrective interventions.

53

54 **Keywords:** Human facial growth; 3D scanning; Morphometrics; Sexual Dimorphism

55

56 **Introduction:**

57 Craniofacial surgery aims to correct congenital and acquired deformities by realigning
58 patients with the 'normal' population. To achieve this, knowledge of the range of
59 normality and a means by which patients can be assessed against this are essential.
60 Our aim in this paper is to develop a statistical model of whole head surface variation
61 based on individuals living in the UK of both sexes, ranging in age from 3-20 years.
62 We explore the extent and nature of changes in the size and shape of the head in this
63 age range, comparing early and later stages of growth and development and assess
64 sexual dimorphism in the sample.

65 Anthropometry of facial soft and hard tissues, has a long history in studies of
66 craniofacial biology and plastic and reconstructive surgery (Howells, 1973; O'Higgins
67 et al., 1990; Farkas, 1994). In craniostyostosis surgery, the cranial index derived from
68 calliper measurements of skull maximum width expressed as a percentage of
69 maximum length is commonly used. Although this is easily measured and repeatable,
70 it captures limited aspects of cranial form and can be misleading as an outcome
71 measure. Such approaches suffer several mensurational and statistical issues
72 (Moyers and Bookstein, 1979; Rohlf, 2000) and are not useful in regions with few
73 recognizable landmarks.

74 To address this, using 3D surface images, correspondences of points among surface
75 meshes are frequently computed using a template landmark configuration close to the
76 average of the population (Blanz and Vetter, 1999), with or without user-specified,
77 anatomically-equivalent landmarks (Paysan et al., 2009). The template is then
78 morphed to the set of surfaces to be landmarked. Examples include the Non-rigid
79 Iterative Closest Points (NICP) algorithm (Amberg et al., 2007) and the Coherent Point

80 Drift (CPD) algorithm (Myronenko and Song, 2010). A recent approach trains a
81 statistical shape model of the human head (Dai et al., 2018), combining CPD with a
82 methodology that employs 'as-rigid-as-possible' deformations (Sorkine and Alexa,
83 2007) to iteratively locate landmarks. This is similar to the sliding semilandmark
84 technique from Geometric Morphometrics (GM), applied in the present study because
85 it explicitly seeks to map developmental homologies. In this, anatomical landmarks
86 guide the 'sliding' of semilandmarks over curves and surfaces to minimise 'bending
87 energy' (local 'error' in semilandmark placement; see Methods).

88 Once surface meshes have been parameterised as sets of corresponding landmarks,
89 models of variation can be derived and used to assess other surface meshes. These
90 generally use approaches based on estimations of shape or size and shape distances
91 derived from generalised Procrustes analysis, principal components analysis and
92 other multivariate methods, as is common in GM studies (Dai et al., 2020).

93 In the paediatric population, assessment of craniofacial form is complicated by
94 dynamic, continuous growth changes. Since congenital craniofacial abnormalities are
95 typically surgically corrected early in childhood, it is vital that surgeons have access to
96 an age and sex appropriate 3D craniofacial model pre- and post-operatively. Currently,
97 there is no widely accepted objective measure of paediatric craniofacial normality. A
98 precise understanding of human ontogeny and sex differences that arise during
99 childhood is essential for generating such a model, and so to understanding
100 craniofacial pathologies and their correction.

101 Between birth and adulthood, sexual dimorphism of craniofacial form becomes
102 apparent. Dimorphic differences between adult male and female soft tissue faces (Dai
103 et al., 2020; Ploumpis et al., 2020) and the craniofacial skeleton are well described

104 (Bulygina et al., 2006; Franklin et al., 2007; O'Higgins et al., 1990; Rosas and Bastir,
105 2002). Principally, males are noted to have prominent chins, jaw angles, supraorbital
106 and nasal regions and relatively reduced cheeks as well as being larger than females.
107 Typically, these changes are linked to hormone associated growth differences with
108 males, for the most part, extending growth and so, form change, relative to females
109 during late puberty. Sex differences have been noted at varying subadult ages; 3 years
110 (Kesterke et al., 2016), 4.7years (Gaži-Čoklica et al., 1997), 6 years (Ferrario et al.,
111 1999) and 14 years (Koudelová et al., 2015) with a recent study (Matthews, 2018)
112 claiming the presence of sexual dimorphism in children as early as 1 year.

113 This study revisits the issues of ontogenetic and sexual variation in craniofacial form
114 using an approach to landmarking and analysis that explicitly respects homology. This
115 ensures that the underlying (distance) metric relates to biologically meaningful
116 differences. We characterise postnatal ontogenetic changes in size and shape and
117 investigate the ontogeny of sexual dimorphism, comparing our findings with those of
118 previous studies. Through this study we demonstrate the efficacy of a statistically and
119 biologically valid approach to such work that can be readily replicated in clinical
120 research using commonly available and inexpensive software tools. These have
121 significant potential in pre- and post-operative surgical management.

122 **Methods:**

123 **Ethics approval:**

124 Ethics approval was granted by Alder-Hey Hospital and The Hull York Medical School.
125 Written informed consent was gained from all volunteers, or their legal guardian if
126 <18years. Consent was to allow the 3D photography of their heads to provide data to

127 assess normal head variation. We confirm adherence to the tenets of the Declaration
128 of Helsinki.

129 **Sample:**

130 The sample comprises Wavefront™ .obj head surface meshes (typically 180K vertices
131 and approx. 360K triangles) from 65 males and 47 females (range 3-20 years; Table
132 1). These were chosen from the sample collected by the *Headspace* (see 'Software,
133 tools and data availability') project in Liverpool from September 2013 – January 2014
134 using a 3dMD five-camera system to capture head geometry. All participants wore
135 smooth, tight fitting latex caps to flatten the hair closely to the scalp. Individuals who
136 had previous craniofacial surgery, declared mixed or unknown ethnicity, bulky hair or
137 errors in their surface data were excluded, thus limiting sources of error as far as
138 possible and focussing on growth within the indigenous local population.

139 **Digitisation:**

140 Developmentally homologous landmarks, curves and surfaces were digitised using an
141 algorithm devised by Bookstein and Green (Bookstein and Green, 1994). This was
142 further developed (Gunz and Mitteroecker, 2013) and incorporated in the EVAN
143 Toolbox for geometric morphometrics (Weber and Bookstein, 2011), which was used
144 in this study.

145 A template was created in the EVAN Toolbox comprising 16 anatomical landmarks
146 (Table 2) and an exemplar head surface mesh with traced curves marked up by 59
147 semilandmarks. The semi-landmark configurations represented the right and left
148 jawlines, the right and left eyebrows and the midline, as well as the surface between
149 curves and landmarks (Fig. 1). To facilitate subsequent interpretation of asymmetry,
150 the template was rendered symmetrical using the method of reflected relabelling

151 (Mardia et al., 2000). Semilandmarks were then warped and projected from the
152 template onto each parent curve or surface in each individual using a triplet of thin
153 plate splines (Bookstein, 1989). The semilandmarks were then slid along curves and
154 over the surface to minimise the bending energy of the thin plate splines with respect
155 to the anatomical landmarks (Bookstein, 1989; Gunz and Mitteroecker, 2013). The
156 full set of 16 anatomical landmarks and 59 semilandmarks was used as the basis of
157 subsequent statistical analyses.

158

159 **Statistical analyses:**

160 The analyses examined growth (changes in size and shape), development (changes
161 in shape over time) and ontogenetic transformation as a whole (changes in size and
162 shape over time) from 3-20 years. For subsequent analyses centroid size (the square
163 root of the sum of squared distances between each landmark and the centroid) was
164 used as measure of scale, and the shape variables are the landmark and
165 semilandmark coordinates after generalised Procrustes analysis (GPA). Analyses of
166 form (shape and size; Mitteroecker et al., 2013) use these shape variables plus the
167 natural logarithm of centroid size (\ln csize) .

168 Changes were assessed for the whole sample using principal components analysis
169 (PCA) and modelled using multivariate regressions, both computed using the EVAN
170 Toolbox. The regressions were repeated for younger (3-10 years) and older (11-20
171 years) subjects and the directions of regression vectors were compared using a
172 permutation test on the angles between them (using the R package Arothron (Profico
173 et al., 2015). Additionally, regressions and tests of angles were repeated for each sex
174 alone. Finally, residual sexual differences in shape from these regressions, after

175 adjusting all individuals to mean age or centroid size, were assessed for significance
176 using a permutation test. The results of these analyses were visualised by warping the
177 template surface mesh between the landmarks and semilandmarks of pairs of
178 surfaces (from the 'reference' to the 'target') derived by warping along principal
179 components or multivariate regression vectors of interest. To facilitate interpretation
180 of how each target surface differs from its reference, the surface mesh was converted
181 into a colour map, representing the change in area of each triangle of the surface mesh
182 between these, using the MapAreaDist in the R package, Arothron (Piras et al., 2020).

183 **Results**

184 Between 3 and 20 years, centroid size and age are strongly associated (Fig. 2; whole
185 sample $r = 0.84$; males $r = 0.88$; females $r = 0.87$; all $p < 0.00001$). Males and females
186 largely overlap, although the oldest males attain greater centroid sizes than females.
187 Additionally, the youngest males appear somewhat smaller than the youngest females
188 leading to the impression that growth vectors may differ but the angle between the sex
189 specific vectors of size regressed on age is not significantly different from 0 (29° ,
190 permutation test $p = 0.69$).

191 A principal components analysis of shape (the coordinates after GPA) was carried out
192 for the whole sample. In Fig. 3., males and females overlie each other except at the
193 positive limit of PC1 where males exceed females in density. Warping of the mean to
194 the limits of PC1 (Fig. 3, insets lower frame) indicates that the shape changes it
195 represents are similar to what we would expect of development, with heads more
196 typical of young adults plotting towards the positive extreme of PC1. Older females
197 tend to have lower PC1 scores than older males, indicating that their morphology is
198 more juvenile-like than that of similarly aged males.

199 A second PCA of form (shape variables plus \ln centroid size) is presented in Fig. 4.
200 As in the PCA of shape (Fig. 3), the positive limit of PC1 shows a greater density of
201 males than females and the warped mean closely resembles the changes in size and
202 shape that would be expected of growth and development, with larger more mature
203 looking individuals plotting towards the upper limit of PC1. As in Fig. 3, older females
204 have lower PC1 scores than older males.

205 In both PCAs there is a suggestion of curvilinearity of ontogenetic trajectories with a
206 change in vector near 10 years of age in higher PCs (PC4, shape; PC5, form, not
207 shown). In Fig. 2, males below 10 years tend to be smaller than females, and larger
208 above 10 years. Additionally, many previous studies have indicated that growth of the
209 head shifts from being dominated by changes in the neurocranium earlier in
210 development and in the face, later. For these reasons we divided the sample into two
211 age cohorts, 3-10 years and 11-20 years, to assess the extent to which ontogenetic
212 vectors change over time.

213 The results of the multivariate regressions of shape on size, shape on age and form
214 on age are presented in Table 3. These were calculated for combined sexes 3-20
215 years, combined sexes 3-10 years and 11-20 years as well as sexes separately for
216 ages 3-10yrs and 11-20 years. All are highly significant ($p < 0.001$), indicating that the
217 sample as whole and each subsample shows significant ontogenetic changes in form
218 over time. The % of total variance in shape, explained by the regression of shape on
219 \ln centroid size in the 3-10 year olds is ~1.5 times as great as that in the 11-20 year
220 olds. Similarly, for the regression of shape on age almost twice as much variance is
221 explained in the younger age group and for form on age, more than twice.

222 The significance of angles between the regression vectors of ontogenetic change in
223 size and shape from Table 3 and are presented in Table 4. In every comparison
224 between age groups there is a significant difference, indicating different allometries,
225 developments and so, ontogenies. The warpings of Fig. 5 indicate that between the
226 ages of 3 and 10 years, changes in head form mainly comprise expansions of the
227 orbital and nasal regions with accompanying smaller expansions in the regions of the
228 cheeks and chin. These contribute to vertical increase in facial height and nasal
229 protuberance. Between the ages of 11 and 20 the focus of facial expansion shifts
230 inferiorly, being concentrated around the lips and chin, which become more prominent.

231 Over the whole period 3-20 years and within each of the age subgroups, there is no
232 significant difference between sexes in the directions of their ontogenetic vectors
233 (Table 4). Table 5 presents further analyses of sexual dimorphism that test the
234 significance of differences (Procrustes shape or form distances). A permutation test is
235 applied after allometric adjustment of each individual by multivariate regression to
236 mean ln centroid size or to ages 7.5 years for the younger, and 15.5 years for the older
237 age groups. Multivariate regression was based on pooled sexes, because the previous
238 analyses (Table 4) showed their vectors do not differ. These tests indicate that there
239 are no significant residual sex differences in shape in the younger age group but, in
240 the older age group, differences are highly significant. The Procrustes form distance
241 between the means of males and females adjusted to age 15.5 (0.0164) is
242 approximately 25% of the total form difference (0.064) between sexes aged 19 and 20
243 years. The Procrustes shape distance (0.0164) between the means of sexes adjusted
244 to the mean ln centroid size is a little over half the total sex shape distance (0.028) for
245 19-20 year olds.

246 Therefore, these residual aspects of sexual dimorphism are small but not unimportant
247 relative to the component of form difference arising from hypermorphosis. They are
248 shown in Fig. 6, magnified by a factor of 10 to facilitate visualisation. After regression
249 adjustment, males relative to females have a more vertically elongated and narrow
250 head. Females possess relatively larger lips and nasal bridge with a more rounded,
251 shorter chin, relatively smaller jaw angles and a philtrum that is less prominent. These
252 differences are common to, but not equally marked in the residuals from the two
253 regressions, indicating that age and size related changes in shape are not quite
254 coincident in the older age groups.

255 **Discussion**

256 Our analyses find no difference in the rate of growth (change in size with age) between
257 sexes but indicate that the oldest males are larger than the oldest females (Fig 2).
258 Regarding shape and form variation, both PCAs (Fig. 3 and 4) indicate that a
259 substantial contributor to young adult craniofacial sexual dimorphism is
260 hypermorphosis; males extend a common trajectory of growth and development into
261 larger size ranges with shape scaling allometrically. These findings reflect similar
262 results from previous studies of soft tissue faces (Kesterke et al., 2016) and the
263 craniofacial skeleton (Bulygina et al., 2006; Franklin et al., 2008; O'Higgins et al., 1990;
264 Rosas and Bastir, 2002).

265 Regression analyses (Table 2) indicate that growth and development are relatively
266 greater sources of variation among 3-10 year olds than among 11-20 year olds.
267 Further, age appears marginally better than size as a predictor of shape than size
268 alone (ignoring allometric effects), which accounts for a major proportion of the
269 observed ontogenetic changes in overall form with age. Angular comparisons of these

270 vectors (Table 4) find no difference in allometry (shape vs size), development (shape
271 vs age), or in how form varies with age among sexes in either age group but very clear
272 differences in all regression vectors between younger (below 10) and older (11-20)
273 age groups.

274 How form changes with age in both age groups is visualised in Fig. 5. In the younger
275 group, changes in head shape mainly comprise expansions of the orbital and nasal
276 regions and to a lesser extent, the cheeks and chin, contributing to increased facial
277 height and nasal protuberance. The focus of change shifts inferiorly between the ages
278 of 11 and 20 to the region of the lips and chin, leading to their becoming more
279 prominent. These findings are consistent with earlier work (Bastir et al., 2006; Enlow,
280 1968) that identified a maturation gradient which results in early completion of
281 neurocranial growth, followed sequentially by the mid and lower face. The gradient
282 likely reflects differences in rate and duration of growth between brain, bone and
283 cartilage (Bastir et al., 2006) with vertical growth linked to intranasal cartilage
284 expansions and chin prominence linked to continuing growth at the mandibular
285 condyles (Enlow and Hans, 1996; Scott, 1954).

286 Finally, while allometric scaling as a consequence of male hypermorphosis underlies
287 a significant proportion of sexual dimorphism in our sample, the regression analyses
288 suggest that some proportion of sexual dimorphism is independent of scaling and
289 temporal extension of growth in males (time hypermorphosis). These aspects are
290 shown in Fig. 6. In this, the differences are magnified 10 times and consist of a more
291 vertically elongated and narrow head in males relative to females and much larger lips
292 and nasal bridge with a more rounded, shorter chin, relatively smaller jaw angles and
293 philtrum in females. These sex differences are significant but the angle between
294 regressions in each sex are insignificant, probably due to limitations of sampling,

295 particularly below 10 years. As such, we cannot determine if these differences arise
296 early, in the neonatal period and are simply carried forward into adulthood, being
297 added to by male hypermorphosis (Ferrario et al., 1999; Gaži-Čoklica et al., 1997;
298 Kesterke et al., 2016; Koudelová et al., 2015), or have arisen through divergence of
299 trajectories

300 The current work contributes to our understanding of how the head grows and
301 develops and was carried out using the readily available Evan Toolbox and R based
302 software for colour maps that is open source. Using these, this research can readily
303 be extended to different populations. Further, with little development it is possible to
304 envisage a semiautomatic tool for scanning and parameterising the heads of patients
305 in the clinical setting with the aim of enhancing diagnosis and treatment of craniofacial
306 growth disorders, as well as characterising site and extent of dysmorphology to enable
307 both surgical planning and outcomes assessment.

308

309 **Software, tools and data availability**

310 The Headspace data are available via the project website, [https://www-](https://www-users.cs.york.ac.uk/~nep/research/Headspace/)
311 [users.cs.york.ac.uk/~nep/research/Headspace/](https://www-users.cs.york.ac.uk/~nep/research/Headspace/). Our VPN for the EVAN toolbox
312 analyses are distributed via <https://www.evan-society.org/>; The template and data can
313 be downloaded from <https://doi.org/10.5281/zenodo.4266269>; The R tool for
314 visualisation of differences in meshes is available on CRAN at [https://CRAN.R-](https://CRAN.R-project.org/package=Arothron)
315 [project.org/package=Arothron](https://CRAN.R-project.org/package=Arothron), the function is localmeshdiff.

316

317

318

319

320 **References**

- 321 Amberg, B., Romdhani, S., Vetter, T., 2007. Optimal step nonrigid ICP algorithms for
322 surface registration, in: 2007 IEEE Conference on Computer Vision and Pattern
323 Recognition. IEEE, pp. 1–8.
- 324 Bastir, M., Rosas, A., O’Higgins, P., 2006. Craniofacial levels and the morphological
325 maturation of the human skull. *J Anat* 209, 637–654.
326 <https://doi.org/10.1111/j.1469-7580.2006.00644.x>
- 327 Blanz, V., Vetter, T., 1999. A morphable model for the synthesis of 3D faces, in:
328 Proceedings of the 26th Annual Conference on Computer Graphics and
329 Interactive Techniques. pp. 187–194.
- 330 Bookstein, F.L., 1989. Principal warps: Thin-plate splines and the decomposition of
331 deformations. *IEEE Transactions on Pattern Analysis & Machine Intelligence*
332 567–585.
- 333 Bookstein, F.L., Green, W.D., 1994. Edgewarp: A flexible program package for
334 biometric image warping in two dimensions, in: *Visualization in Biomedical*
335 *Computing 1994*. International Society for Optics and Photonics, pp. 135–147.
- 336 Bulygina, E., Mitteroecker, P., Aiello, L., 2006. Ontogeny of facial dimorphism and
337 patterns of individual development within one human population. *Am J Phys*
338 *Anthropol* 131, 432–443. <https://doi.org/10.1002/Ajpa.20317>
- 339 Dai, H., Pears, N., Smith, W., Duncan, C., 2020. Statistical Modeling of Craniofacial
340 Shape and Texture. *International Journal of Computer Vision* 128, 547–571.
- 341 Dai, H., Pears, N., Smith, W., Duncan, C., 2018. Symmetric Shape Morphing for 3D
342 Face and Head Modelling. Presented at the Automatic Face & Gesture
343 Recognition (FG 2018), 2018 13th IEEE International Conference on, IEEE, pp.
344 91–97.

345 Enlow, D.H., 1968. The human face: an account of the postnatal growth and
346 development of the craniofacial skeleton. Hoeber Medical Division, Harper &
347 Row.

348 Enlow, D.H., Hans, M.G., 1996. Essentials of Facial Growth. W. B. Saunders
349 Company, Philadelphia.

350 Farkas, L.G., 1994. Anthropometry of the Head and Face. Raven Pr.

351 Ferrario, V.F., Sforza, C., Poggio, C.E., Schmitz, J.H., 1999. Soft-tissue facial
352 morphometry from 6 years to adulthood: a three-dimensional growth study
353 using a new modeling. Plastic and reconstructive surgery 103, 768–778.

354 Franklin, D., O’Higgins, P., Oxnard, C.E., 2008. Sexual dimorphism in the mandible of
355 indigenous South Africans: A geometric morphometric approach. S Afr J Sci
356 104, 101–106.

357 Franklin, D., Oxnard, C.E., O’Higgins, P., Dadour, I., 2007. Sexual dimorphism in the
358 subadult mandible: Quantification using geometric morphometrics. J Forensic
359 Sci 52, 6–10. <https://doi.org/10.1111/j.1556-4029.2006.00311.x>

360 Gaži-Čoklica, V., Muretić, Ž., Brčić, R., Kern, J., Miličić, A., 1997. Craniofacial
361 parameters during growth from the deciduous to permanent dentition—a
362 longitudinal study. European journal of orthodontics 19, 681–689.

363 Gunz, P., Mitteroecker, P., 2013. Semilandmarks: a method for quantifying curves and
364 surfaces. Hystrix, the Italian journal of mammalogy 24, 103–109.

365 Howells, W.W., 1973. Cranial variation in man. Papers of the Peabody Museum of
366 Archaeology and Ethnology, Harvard University 67. Cambridge. Mass.

367 Kesterke, M.J., Raffensperger, Z.D., Heike, C.L., Cunningham, M.L., Hecht, J.T., Kau,
368 C.H., Nidey, N.L., Moreno, L.M., Wehby, G.L., Marazita, M.L., 2016. Using the

369 3D Facial Norms Database to investigate craniofacial sexual dimorphism in
370 healthy children, adolescents, and adults. *Biology of sex differences* 7, 23.

371 Koudelová, J., Brůžek, J., Cagáňová, V., Krajíček, V., Velemínská, J., 2015.
372 Development of facial sexual dimorphism in children aged between 12 and 15
373 years: a three-dimensional longitudinal study. *Orthodontics & craniofacial*
374 *research* 18, 175–184.

375 Mardia, K.V., Bookstein, F.L., Moreton, I.J., 2000. Statistical assessment of bilateral
376 symmetry of shapes. *Biometrika* 285–300.

377 Matthews, H.S., 2018. Changing the face of craniofacial growth curves: modelling
378 growth and sexual dimorphism in children and adolescents using spatially
379 dense 3D image analysis.

380 Mitteroecker, P., Gunz, P., Windhager, S., Schaefer, K., 2013. A brief review of shape,
381 form, and allometry in geometric morphometrics, with applications to human
382 facial morphology. *Hystrix* 24, 59–66. <https://doi.org/10.4404/hystrix-24.1-6369>

383 Moyers, R.E., Bookstein, F.L., 1979. The inappropriateness of conventional
384 cephalometrics. *American journal of orthodontics* 75, 599–617.

385 Myronenko, A., Song, X., 2010. Point set registration: Coherent point drift. *IEEE*
386 *transactions on pattern analysis and machine intelligence* 32, 2262–2275.

387 O’Higgins, P., Moore, W.J., Johnson, D.R., McAndrew, T.J., Flinn, R.M., 1990.
388 Patterns of cranial sexual dimorphism in certain groups of extant hominoids.
389 *Journal of Zoology* 222, 399–420.

390 Paysan, P., Knothe, R., Amberg, B., Romdhani, S., Vetter, T., 2009. A 3D face model
391 for pose and illumination invariant face recognition, in: 2009 Sixth IEEE
392 International Conference on Advanced Video and Signal Based Surveillance.
393 Ieee, pp. 296–301.

394 Piras, P., Profico, A., Pandolfi, L., Raia, P., Di Vincenzo, F., Mondanaro, A.,
395 Castiglione, S., Varano, V., 2020. Current options for visualization of local
396 deformation in modern shape analysis applied to paleobiological case studies.
397 *Frontiers in Earth Science* 8, 66.

398 Ploumpis, S., Ververas, E., O'Sullivan, E., Moschoglou, S., Wang, H., Pears, N.,
399 Smith, W., Gecer, B., Zafeiriou, S.P., 2020. Towards a complete 3D morphable
400 model of the human head. *IEEE Transactions on Pattern Analysis and Machine*
401 *Intelligence*.

402 Profico, A., Veneziano, A., Melchionna, M., Piras, P., Raia, P., 2015. Arothron: R
403 functions for geometric morphometrics analyses. R package version 314.

404 Rohlf, F.J., 2000. On the use of shape spaces to compare morphometric methods.
405 *Hystrix, the Italian Journal of Mammalogy* 11, 9–25.

406 Rosas, A., Bastir, M., 2002. Thin-plate spline analysis of allometry and sexual
407 dimorphism in the human craniofacial complex. *American Journal of Physical*
408 *Anthropology* 117, 236–245. <https://doi.org/10.1002/ajpa.10023>

409 Scott, J.H., 1954. The growth of the human face. *Proceedings of the Royal Society of*
410 *Medicine* 47, 91–100.

411 Sorkine, O., Alexa, M., 2007. As-rigid-as-possible surface modeling, in: *Symposium*
412 *on Geometry Processing*. pp. 109–116.

413 Weber, G.W., Bookstein, F.L., 2011. *Virtual Anthropology - A Guide for a New*
414 *Interdisciplinary Field*. Springer-Verlag, Wien.

415

416

417

418 **Legends for figures**

419

420 **Figure 1:** top row, left: The fixed landmarks (see Table 1), curves and surface
421 measured on each head. Top row, right: the same landmarks, curves and surfaces
422 with semilandmarks. Bottom row: frontal and lateral views of a fully parameterised
423 head.

424 **Figure 2:** Growth of the head; Females, black circles, Males, crosses.

425 **Figure 3:** PCA of shape using the whole sample, ages 3-20. PC1 accounts for 32%
426 of the total variance and PC2 for 11%. Females, black circles, Males, crosses.

427 **Figure 4:** PCA of form using the whole sample, ages 3-20. PC1 accounts for 77% of
428 the total variance and PC2 for 4%. Females, black circles, Males, crosses.

429 **Figure 5:** Visualisation of the changes from 3-10-20 years (left, middle, right) from
430 multivariate regression of form (shape and size) on age. The head colour maps
431 indicate the relative expansion or contraction in the area of surface regions between
432 3 and 10 years (middle) and between 11 and 20 years (right).

433 **Figure 6:** Visualisations of residual sex dimorphism in shape (differences between sex
434 means) after warping all individuals between 11 and 20 years to age 15.5 years (top)
435 and to ln of the mean centroid size (bottom). The warping of each head from the sex
436 mean is exaggerated by a factor of 5 and so the differences between heads appear
437 10x greater than in reality.

438

439 **Table legends:**

440 **Table 1:** Individuals included in this study by age and sex

441 **Table 2:** Definitions of fixed facial landmarks

442 **Table 3:** Multivariate regressions of shape on ln centroid size and age, and of form on
443 age within each age group with sexes separate and combined. All regressions are
444 significant as assessed using a permutation test.

445 **Table 4:** Comparisons of ontogenetic trajectories from multivariate regressions of
446 shape on ln centroid size and age, and of form on age. The magnitudes and
447 significances of the angles between trajectories are presented for comparisons
448 between age groups and sexes. Significance was assessed using a permutation test,
449 significant differences in bold.

450 **Table 5:** The degree and significance of sexual dimorphism in shape in each age
451 group before and after adjusting data to mean ln centroid size or ages, 7.5 years (3-
452 10 age group), 15.5 years (11-20 age group). Dimorphism is quantified using
453 distances, D, which are Procrustes shape distances (upper row) and Procrustes form
454 distances (lower row). Significance was assessed using a permutation test, significant
455 differences in bold.

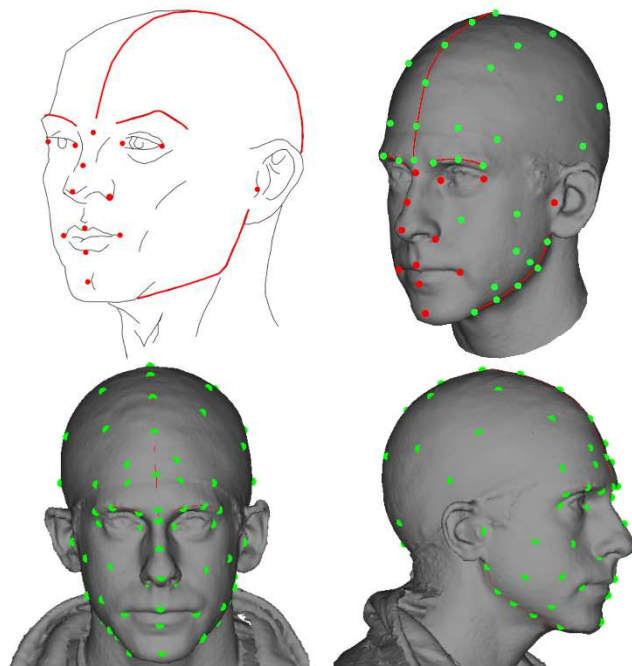
456

457

458

459

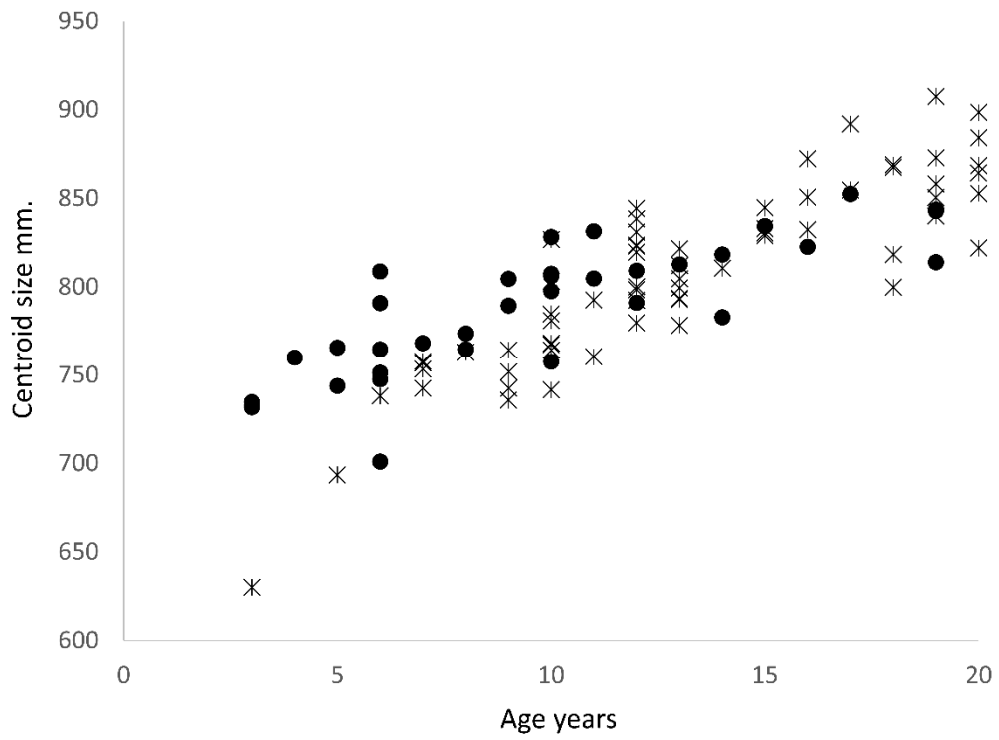
460



461

462 **Figure 1:** top row, left: The fixed landmarks (see Table 1), curves and surface
463 measured on each head. Top row, right: the same landmarks, curves and surfaces
464 with semilandmarks. Bottom row: frontal and lateral views of a fully parameterised
465 head.

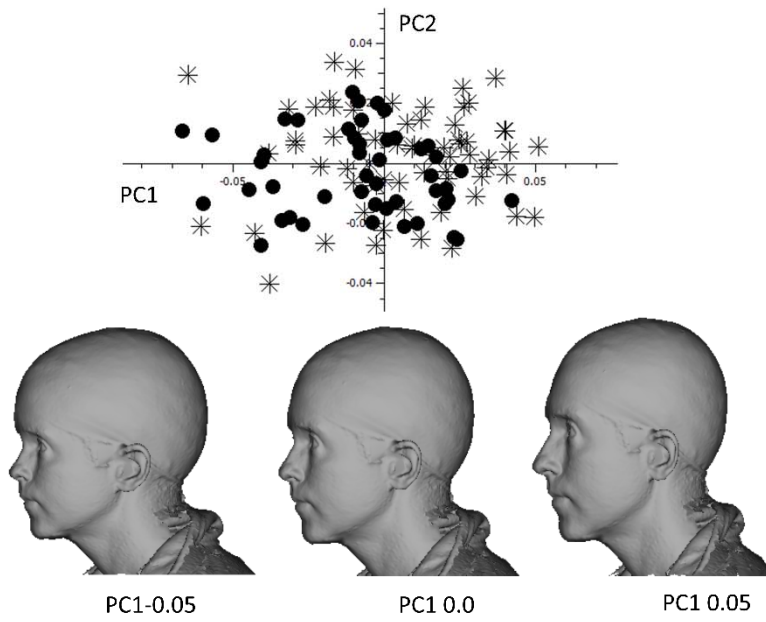
466



467

468 **Figure 2:** Growth of the head; Females, black circles, Males, crosses.

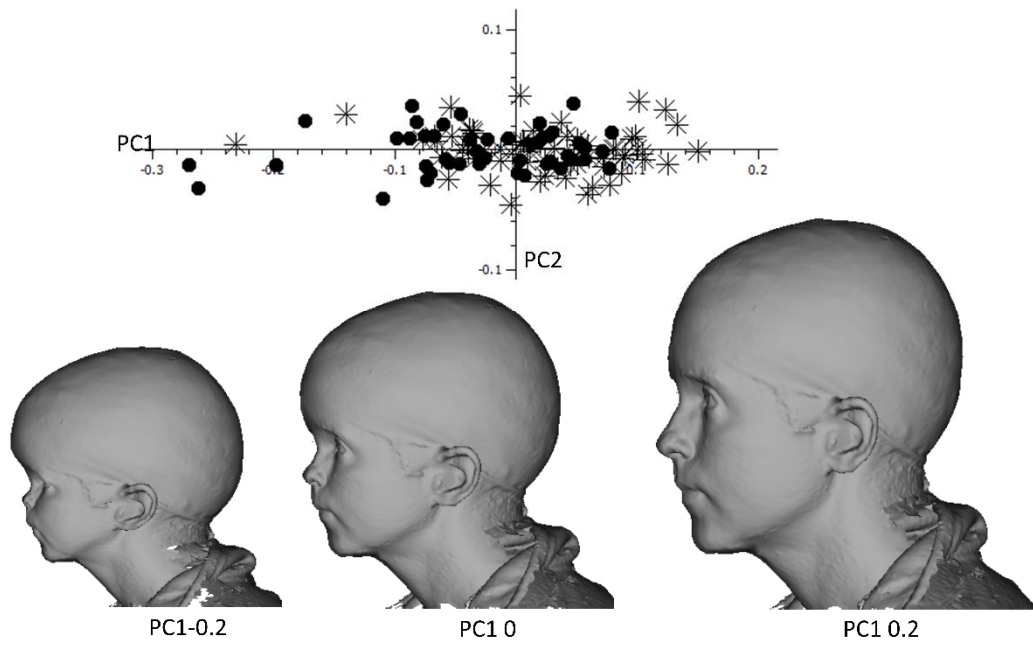
469



470

471 **Figure 3:** PCA of shape using the whole sample, ages 3-20. PC1 accounts for 32%
 472 of the total variance and PC2 for 11%. Females, black circles, Males, crosses.

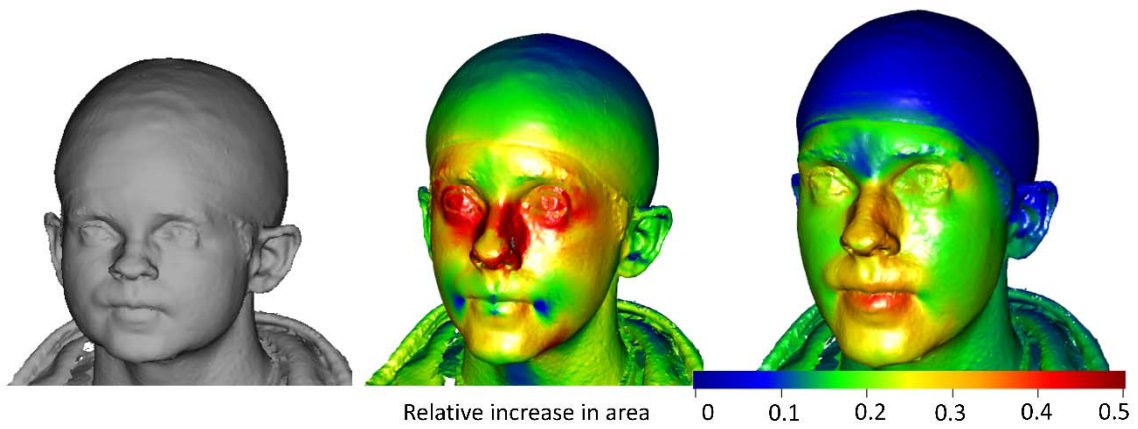
473



474

475 **Figure 4:** PCA of form using the whole sample, ages 3-20. PC1 accounts for 77% of
 476 the total variance and PC2 for 4%. Females, black circles, Males, crosses.

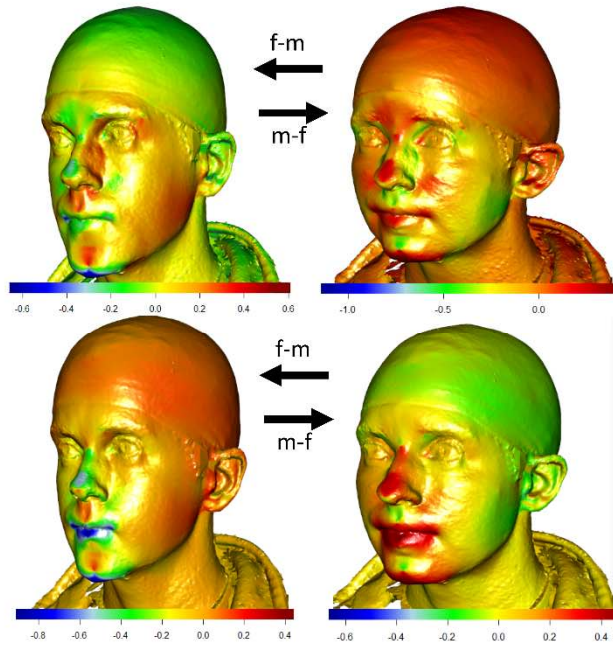
477



478

479 **Figure 5:** Visualisation of the changes from 3-10-20 years (left, middle, right) from
480 multivariate regression of form (shape and size) on age. The head colour maps
481 indicate the relative expansion or contraction in the area of surface regions between
482 3 and 10 years (middle) and between 11 and 20 years (right).

483



484

485 **Figure 6:** Visualisations of residual sex dimorphism in shape (differences between sex
 486 means) after warping all individuals between 11 and 20 years to age 15.5 years (top)
 487 and to ln of the mean centroid size (bottom). The warping of each head from the sex
 488 mean is exaggerated by a factor of 5 and so the differences between heads appear
 489 10x greater than in reality.

490

Age Yrs.	f	m
3	3	1
4	1	
5	2	1
6	6	1
7	1	4
8	2	2
9	2	4
10	5	8
11	3	2
12	2	10
13	1	7
14	2	1
15	1	4
16	1	3
17	1	2
18		4
19	8	5
20	6	6

491 **Table 1:** Individuals included in this study by age and sex

No.	Landmark definition
1 & 3	Medial canthus
2 & 4	Lateral canthus
5	Nasal bridge
6	Middle of nose
7	Tip of nose
8 & 9	Corner of mouth
10	Middle of cupid's bow upper lip
11	Middle of bottom lip
12	Tip of chin
13 & 14	Tragus
15 & 16	Lateral nasal alar rim

Multivariate regressions	Shape v Ln centroid Size			Shape v age		Form v age	
	n	(% Var. exp.)	significance <i>p</i>	(% Var. exp.)	significance <i>p</i>	(% Var. exp.)	significance <i>p</i>
Combined sexes 3-20	112	20.04	<0.001	20.89	<0.001	56.06	<0.001
Combined sexes 3-10	43	12.76	<0.001	16.79	<0.001	49.23	<0.001
3-10 male	21	16.95	<0.001	19.47	<0.001	47.36	<0.001
3-10 female	22	13.78	<0.002	19.9	<0.001	46.35	<0.001
Combined sexes 11-20	69	9.03	<0.001	9.83	<0.001	21.25	<0.001
11-20 male	44	9.88	<0.001	14.4	<0.001	32.38	<0.001
11-20 female	25	9.41	0.003	10.66	<0.001	27.57	<0.001

499

500 **Table 3:** Multivariate regressions of shape on ln centroid size and age, and of form on
501 age within each age group with sexes separate and combined. All regressions are
502 significant as assessed using a permutation test.

503

504

505

Ontogenetic vector comparisons	Shape vs. size		Shape vs. age		Form vs age	
	angle ^o	P	angle ^o	p	angle ^o	p
between ages 3-10 and 11-20						
3-10 female vs 11-20 female	72	<0.001	64	<0.001	27	<0.001
3-10 female vs 11-20 male	53	<0.001	48	<0.001	21	<0.001
3-10 male vs 11-20 male	62	<0.001	67	<0.001	29	<0.001
3-10 male vs 11-20 female	69	<0.001	78	<0.001	33	<0.001
combined sexes 3-10 vs 11-20	49	<0.001	61	<0.001	26	<0.001
between the sexes						
3-20 female vs 3-20 male	23	0.379	22	0.223	8	0.195
3-10 female vs 3-10 male	48	0.417	45	0.181	17	0.264
11-20 female vs 11-20 male	47	0.181	43	0.278	21	0.561

506

507 **Table 4:** Comparisons of ontogenetic trajectories from multivariate regressions of
 508 shape on ln centroid size and age, and of form on age. The magnitudes and
 509 significances of the angles between trajectories are presented for comparisons
 510 between age groups and sexes. Significance was assessed using a permutation test,
 511 significant differences in bold.

512

513

514

Sexual dimorphism	age 3-10		age 11-20	
	D	p	D	p
Shape adjusted to mean ln centroid size	0.00963	0.888	0.0164	0.004
Form adjusted to 7.5/15.5 years	0.01061	0.752	0.0164	0.001

515

516 **Table 5:** The degree and significance of sexual dimorphism in shape in each age
517 group before and after adjusting data to mean ln centroid size or ages, 7.5 years (3-
518 10 age group), 15.5 years (11-20 age group). Dimorphism is quantified using
519 distances, D, which are Procrustes shape distances (upper row) and Procrustes form
520 distances (lower row). Significance was assessed using a permutation test, significant
521 differences in bold.

522